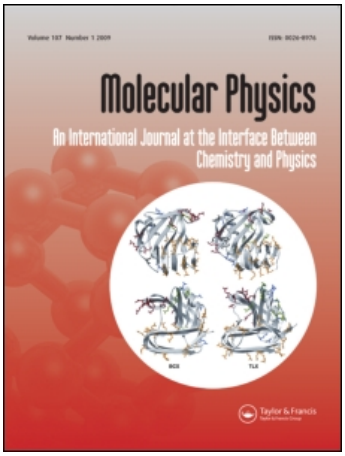

Molecular Physics
Publication details, including instructions for authors and subscription information:
http://www.informaworld.com/smpp/title~content=t713395160

High resolution solution state double quantum spectroscopy of two-spin-1 AX systems and mimics

S. VENKATA RAMAN; N. CHANDRAKUMAR

Online publication date: 03 December 2010

To cite this Article RAMAN, S. VENKATA and CHANDRAKUMAR, N.(1997) 'High resolution solution state double quantum spectroscopy of two-spin-1 AX systems and mimics', Molecular Physics, 90: 5, 855 — 868
To link to this Article: DOI: 10.1080/002689797172192
URL: http://dx.doi.org/10.1080/002689797172192

MOLECULAR PHYSICS, 1997, VOL. 90, NO. 5, 855–868

High resolution solution state double quantum spectroscopy of two-spin-1 AX systems and mimics

By S. VENKATA RAMAN and N. CHANDRAKUMAR

Laboratory of Chemical Physics, Central Leather Research Institute, Adayaru, Chennai-600 020, Tamil Nadu, India

(*Received 19 August 1996; accepted 1 November 1996*)

Double quantum spectroscopy (DQS) of the two-spin-1 AX system in the liquid state is investigated theoretically. The two kinds of double quantum coherence (DQC) that arise are studied and expressions are given for their evolution under weak scalar coupling and chemical shifts. A one-dimensional double quantum J (DQJ) filter sequence for the separation of the two kinds of DQC is introduced. Analytical expressions are given for the spin response to the general two-dimensional DQS sequence, for an arbitrary reconversion pulse flip angle β. A detailed investigation of the coherence transfer (CT) amplitudes has been carried out by computer simulation of CT amplitudes as a function of β. The differences in the behaviour of CT amplitudes of one-spin DQC, 'outer' and 'central' components of two-spin DQCs are discussed. Optimum flip angles for maximizing sensitivity of N-type, P-type and pure phase double quantum spectra of this system are deduced. The detailed predictions are borne out by recently published experimental work on two-spin-1 AX systems, as well as our studies on a mimic arrangement, viz., a spin-1/2 A_2X_2 system.

1. Introduction

The NMR of spin-1 systems has proved to be of fundamental significance in a range of investigations of molecular structure and dynamics [1–19]. For solution state structure elucidation, techniques such as heteronuclear polarization transfer and homonuclear COSY optimized for small couplings have been employed successfully [14, 15]. Recently, it has been shown that solution state rotating frame coherence transfer (TOCSY) is superior to the laboratory frame counterpart in terms of its efficiency because: (i) unlike coherence transfer in weakly coupled spin-1 systems in laboratory frame experiments, the state with $m_I = 0$ also takes part in rotating frame coherence transfer experiments; and (ii) the transfer of coherence is in-phase [16]. More recently, it has been shown that solution state multiple quantum spectroscopy of scalar coupled spin-1 systems gives unique information on molecular structure. In particular, triple quantum spectroscopy reveals three-spin connectivity as well as the direct connectivities of the system [17], while double quantum spectroscopy (DQS) [17–19] reveals both two-spin double quantum peaks that delineate direct spin connectivities, as well as one-spin double quantum peaks, which exhibit amplified couplings. These features of spin-1 DQS have been exploited recently to measure unresolved homonuclear couplings in deuterium NMR and also to deduce organolithium cluster sizes in the solution state [13, 19].

In this work we make a detailed analysis of the solution state DQS of the two-spin-1 AX system. In the theory section we discuss briefly the preparation of the two kinds of double quantum coherences (DQC), viz., one-spin DQC and two-spin DQC. We give expressions for their shift refocused evolution under weak coupling and introduce a spectral editing strategy to separate the two kinds of DQCs. We also give expressions for 2D-DQ evolution under the free precession Hamiltonian of such a system and consider the effects of a reconversion (mixing or transfer) pulse of arbitrary flip angle β. Further, we analyse the coherence transfer (CT) to individual coherences using the rotation matrix approach, and discuss the behaviour of the CT amplitude for small values of β. In the simulation section we present simulations of the CT amplitude as a function of β and discuss the salient features of the CT process as seen from the simulations. We discuss also the optimal flip angles for echo/anti-echo selection and for pure phase spectroscopy. In the experimental and discussion section we present experimental evidence for the theoretical predictions, citing both the recent spin-1 findings and our work with a spin-1/2 A_2X_2 system that is a two-spin-1 AX mimic for our purposes.

0026–8976/97 $12·00

2. Theory

2.1. *Preparation of DQC*

A cluster of spin-coupled spin-1 nuclei exhibits two kinds of double quantum excitation. One, familiar from spin-1/2 DQS [20], corresponds to correlated single quantum flips of two coupled spins; this therefore may be termed two-spin double quantum excitation, and corresponds to type I peaks in spin-1/2 DQS. The second originates in the fact that a spin 1 is a three-level system; this may hence be termed one-spin double quantum excitation. The latter corresponds in fact to the type II DQC of a pair of equivalent spins-1/2. The standard double quantum preparation sequence [17, 18, 23, 24], viz., $90_x - \tau/2 - 180_x - \tau/2 - 90_x$, results in excitation of both one-spin DQC as well as two-spin DQC when applied to a two-spin-1 system IS; this can be seen from the density matrix that results at the end of the double quantum preparation sandwich:

$$\begin{aligned}
I_z + S_z &\xrightarrow{90_x} -(I_y + S_y) \xrightarrow{180_x} I_y + S_y \\
I_y + S_y &\xrightarrow{2\pi J I_z S_z \tau} (c_{2J} - 1)(I_y S_z^2 + I_z^2 S_y) \\
&\quad - s_{2J}(I_x S_z + I_z S_x) + I_y + S_y \\
&\xrightarrow{90_x} (c_{2J} - 1)(I_z S_y^2 + I_y^2 S_z) \\
&\quad + s_{2J}(I_x S_y + I_y S_x) + I_z + S_z \\
&\equiv \tfrac{1}{2}(c_{2J} - 1)(I_z(S_y^2 - S_x^2) + (I_y^2 - I_x^2)S_z) \\
&\quad + s_{2J}(I_x S_y + I_y S_x) \\
&\quad + c_{2J}(I_z + S_z) - \tfrac{1}{2}(c_{2J} - 1)(I_z S_z^2 + I_z^2 S_z), \qquad (1)
\end{aligned}$$

where $c_{2J} = \cos 2\pi J\tau$ and $s_{2J} = \sin 2\pi J\tau$.

The first term of the last member corresponds to one-spin DQC of phase x, while the second term corresponds to two-spin DQC of phase y; the third and fourth terms represent longitudinal order. It can be seen that the amplitude of one-spin DQC is maximized at the preparation time $\tau = 1/(2J)$, at which point the two-spin DQC in fact vanishes. This offers immediate scope for the selective preparation of one-spin DQC with this choice of the preparation time. On the other hand, the amplitude of two-spin DQC is a maximum at $\tau = 1/(4J)$; note, however, that one-spin DQC does not vanish for this value of τ; in fact its amplitude at this point equals one half the amplitude of two-spin DQC. Clearly, no simple preparation strategy would suppress one-spin DQC selectively.

2.2. *Separation of one-spin DQC from two-spin DQC*

We examine next the evolution of the two DQCs under weak homonuclear coupling alone. We have for two-spin DQC:

$$\begin{aligned}
I_x S_y + I_y S_x &\xrightarrow{2\pi J I_z S_z t} \tfrac{1}{2}(c_2 + 1)(I_x S_y + I_y S_x) \\
&\quad + \tfrac{1}{2}(c_2 - 1)([I_z, I_x]_+ [S_y, S_z]_+ \\
&\quad + [I_y, I_z]_+ [S_z, S_x]_+) \\
&\quad + \tfrac{1}{2}s_2([I_y, I_z]_+ S_y + I_y[S_z, S_y]_+ \\
&\quad - [I_z, I_x]_+ S_x - I_x[S_z, S_x]_+), \qquad (2)
\end{aligned}$$

where $c_2 = \cos 2\pi J t$ and $s_2 = \sin 2\pi J t$. For the evolution of one-spin DQC under coupling, on the other hand, we find:

$$\begin{aligned}
I_z(S_y^2 - S_x^2) + (I_y^2 - I_x^2)S_z &\xrightarrow{2\pi J I_z S_z t} \\
c_4(I_z(S_y^2 - S_x^2) + (I_y^2 - I_x^2)S_z) \\
- s_4(I_z^2[S_x, S_y]_+ + [I_x, I_y]_+ S_z^2), \qquad (3)
\end{aligned}$$

where $c_4 = \cos 4\pi J t$ and $s_4 = \sin 4Jt$.

Based on the properties displayed in equations (2) and (3) we introduce here a simple 1D experiment, viz., the double quantum J filter; with this sequence we can separate the two kinds of DQC. The DQJ filter sequence is given in figure 1. Computing the effect of the final 90°_x pulse, proceeding from equations (2) and (3) we have the following expression for the observable terms in the resultant density matrix:

$$\begin{aligned}
&-\tfrac{1}{2}s_{2J}(\cos 2\pi J t_1 + 1)(I_x S_z + I_z S_x) \\
&\quad - \tfrac{1}{2}(c_{2J} - 1)\cos 4\pi J t_1 (I_y(\mathbf{1} - \tfrac{3}{2}S_z^2) + (\mathbf{1} - \tfrac{3}{2}I_z^2)S_y), \qquad (4)
\end{aligned}$$

and these result exclusively from the first term of each of equations (2) and (3), respectively.

The multiplet pattern that results on selection of two-spin DQC by the choice $t_1 = (2n + 1)/8J$ is thus an anti-phase $(-1, 0, 1)$ doublet with a missing central component. On the other hand, the pattern that results on reconversion following the selection of one-spin DQC by the choice $t_1 = (2n + 1)/2J$ is a $(-1, 2, -1)$ triplet.

Note, incidentally, that the proposed sequence is analogous in form to the spin filter sequence [21, 22] known in spin-1/2 work; however, no t_1 averaging is involved in our application.

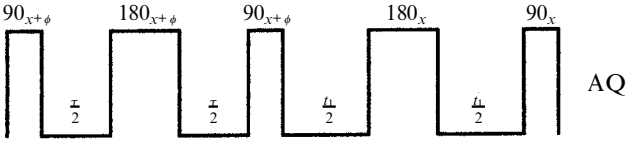

Figure 1. Pulse sequence for the DQJ filter experiment. ϕ is stepped through the standard double quantum phase cycle with concomitant phase alternation of the receiver.

2.3. *2D-DQS for a 90° reconversion pulse*

For the general 2D double quantum evolution without a refocusing pulse, i.e., evolution under the free precession Hamiltonian with weak coupling and chemical shifts, proceeding from equations (2) and (3) we have for two-spin DQC:

$$\begin{aligned}
I_xS_y + I_yS_x \xrightarrow{(\delta_I I_z + \delta_S S_z + 2\pi J I_z S_z)t_1} & \tfrac{1}{4}(\cos(\Sigma + 2\pi J)t_1 \\
& + \cos(\Sigma - 2\pi J)t_1 + 2\cos(\Sigma t_1))(I_xS_y + I_yS_x) \\
& + \tfrac{1}{4}(\sin(\Sigma + 2\pi J)t_1 + \sin(\Sigma - 2\pi J)t_1 \\
& + 2\sin(\Sigma t_1))(I_yS_y - I_xS_x) \\
& + \tfrac{1}{4}(\cos(\Sigma + 2\pi J)t_1 + \cos(\Sigma - 2\pi J)t_1 \\
& - 2\cos(\Sigma t_1))(\{I_z, I_x\}_+\{S_y, S_z\}_+ + \{I_y, I_z\}_+\{S_z, S_x\}_+) \\
& + \tfrac{1}{4}(\sin(\Sigma + 2\pi J)t_1 + \sin(\Sigma - 2\pi J)t_1 \\
& - 2\sin(\Sigma t_1))(\{I_y, I_z\}_+\{S_z, S_y\}_+ - \{I_z, I_x\}_+\{S_x, S_z\}_+) \\
& + \tfrac{1}{4}(\sin(\Sigma + 2\pi J)t_1 - \sin(\Sigma - 2\pi J)t_1) \\
& \times (\{I_x, I_z\}_+ S_x + I_x\{S_z, S_x\}_+ - \{I_z, I_y\}_+ S_y - I_y\{S_z, S_y\}_+) \\
& + \tfrac{1}{4}(\cos(\Sigma + 2\pi J)t_1 - \cos(\Sigma - 2\pi J)t_1) \\
& \times (\{I_x, I_z\}_+ S_y + I_y\{S_z, S_x\}_+ + \{I_z, I_y\}_+ S_x + I_x\{S_z, S_y\}_+),
\end{aligned} \tag{5}$$

where $\Sigma = \delta_I + \delta_S$. For one-spin DQC we have, on the other hand:

$$\begin{aligned}
I_z(S_y^2 - S_x^2) + (I_y^2 - I_x^2)S_z \xrightarrow{(\delta_I I_z + \delta_S S_z + 2\pi J I_z S_z)t_1} & \\
& + \tfrac{1}{2}\{(\cos(2\delta_I + 4\pi J)t_1 + \cos(2\delta_I - 4\pi J)t_1)((I_y^2 - I_x^2)S_z) \\
& + (\cos(2\delta_S + 4\pi J)t_1 + \cos(2\delta_S - 4\pi J)t_1)(I_z(S_y^2 - S_x^2))\} \\
& - \tfrac{1}{2}\{(\sin(2\delta_S + 4\pi J)t_1 + \sin(2\delta_S - 4\pi J)t_1)(I_z\{S_x, S_y\}_+) \\
& + (\sin(2\delta_I + 4\pi J)t_1 + \sin(2\delta_I - 4\pi J)t_1)(\{I_x, I_y\}_+ S_z)\} \\
& - \tfrac{1}{2}\{(\sin(2\delta_I + 4\pi J)t_1 - \sin(2\delta_I - 4\pi J)t_1)(\{I_x, I_y\}_+ S_z^2) \\
& + (\sin(2\delta_S + 4\pi J)t_1 - \sin(2\delta_S - 4\pi J)t_1)(I_z^2\{S_x, S_y\}_+)\} \\
& - \tfrac{1}{2}\{(\cos(2\delta_I + 4\pi J)t_1 - \cos(2\delta_I - 4\pi J)t_1)((I_y^2 - I_x^2)S_z^2) \\
& + (\cos(2\delta_S + 4\pi J)t_1 - \cos(2\delta_S - 4\pi J)t_1)(I_z^2(S_y^2 - S_x^2))\}.
\end{aligned} \tag{6}$$

Here, the anti-commutator $\{A, B\}_+$ denotes $(AB + BA)$.

Note from equations (5) and (6) that while the one-spin DQC is a doublet in F_1 without a 'central' component, the two-spin DQC is a triplet in F_1 with a 'central' component which is independent of J. This is to be compared with the spin-1/2 system, the DQC of which is independent of J. The absence of a 'central' component in one-spin DQC results directly from the fact that it was prepared anti-phase with respect to the coupling to the second spin.

On reconversion with a 90°_x pulse, proceeding from equations (5) and (6) the observable terms of the resultant density matrix for two-spin double quantum coherence are:

$$\begin{aligned}
s_{2J}(I_xS_y + I_yS_x) \xrightarrow{(\delta_I I_z + \delta_S S_z + 2\pi J I_z S_z)t_1, 90^\circ_x} & \\
& \tfrac{1}{4}s_{2J}(\cos(\delta_I + \delta_S + 2\pi J)t_1 + \cos(\delta_I + \delta_S - 2\pi J)t_1 \\
& + 2\cos(\delta_I + \delta_S)t_1)(I_xS_z + I_zS_x).
\end{aligned} \tag{7}$$

These terms arise exclusively from the first term of equation (5). It can be seen from equation (7) that the multiplet pattern in F_1 is an in-phase $(1, 2, 1)$ cosine triplet with a splitting of J, and the pattern in F_2 is a $(-1, 0, 1)$ anti-phase doublet.

The observable terms of the resultant density matrix in case of one-spin DQC are given by:

$$\begin{aligned}
\tfrac{1}{2}(c_{2J} - 1)(I_z(S_y^2 - S_x^2) + (I_y^2 - I_x^2)S_z) \xrightarrow{(\delta_I I_z + \delta_S S_z + 2\pi J I_z S_z)t_1, 90^\circ_x} & \\
\tfrac{1}{2}(c_{2J} - 1)\left\{\begin{array}{l} \tfrac{1}{2}(\cos(2\delta_S + 4\pi J)t_1 + \cos(2\delta_S - 4\pi J)t_1)(I_y(\mathbf{1} - \tfrac{3}{2}S_z^2)) \\ +\tfrac{1}{2}(\cos(2\delta_I + 4\pi J)t_1 + \cos(2\delta_I - 4\pi J)t_1)((\mathbf{1} - \tfrac{3}{2}I_z^2)S_y) \end{array}\right\}.
\end{aligned} \tag{8}$$

These terms arise exclusively from the first term of equation (6). It is clear from equation (8) that for one-spin DQC the multiplet pattern is an in-phase cosine $(1, 0, 1)$ doublet in F_1 with missing central component, resulting in a multiplet splitting of $4J$. Note that this is four times the splitting observed in the single quantum spectrum. The F_2 multiplet pattern is an anti-phase $(-1, 2, -1)$ triplet.

2.4. *Response to reconversion pulse of arbitrary flip angle*

In order to characterize the general case of an arbitrary reconversion pulse flip angle β, as well as the resulting 2D-DQ spectra, we give below the observable terms in the density matrix in such a case. For two-spin DQC we find:

$$\begin{aligned}
I_xS_y + I_yS_x \xrightarrow{(\delta_I I_z + \delta_S S_z + 2\pi J I_z S_z)t_1, \beta_x, \mathrm{obs}} & \\
& \tfrac{1}{4}(\cos(\delta_I + \delta_S + 2\pi J)t_1 + \cos(\delta_I + \delta_S - 2\pi J)t_1 \\
& + 2\cos(\delta_I + \delta_S)t_1)(I_xS_z + I_zS_x)\sin\beta \\
& + \tfrac{1}{4}(\sin(\delta_I + \delta_S + 2\pi J)t_1 + \sin(\delta_I + \delta_S - 2\pi J)t_1 \\
& + 2\sin(\delta_I + \delta_S)t_1)(I_yS_z + I_zS_y)\sin\beta\cos\beta \\
& + \tfrac{1}{4}(\sin(\delta_I + \delta_S + 2\pi J)t_1 - \sin(\delta_I + \delta_S - 2\pi J)t_1 \\
& - 2\cos(\delta_I + \delta_S)t_1)((\mathbf{2} - 3I_z^2)S_y \\
& + I_y(\mathbf{2} - 3S_z^2))\sin\beta\cos^2\beta.
\end{aligned} \tag{9}$$

The observable terms in the case of one-spin DQC, on

the other hand, are given by:

$$I_z(S_y^2 - S_x^2) + (I_y^2 - I_x^2)S_z \xrightarrow{(\delta_I I_z + \delta_S S_z + 2\pi J I_z S_z)t_1, \beta_x, \text{obs}} \rightarrow$$
$$\tfrac{1}{2}(\cos(2\delta_I + 4\pi J)t_1 + \cos(2\delta_I - 4\pi J)t_1)((2 - 3I_z^2)S_y)\sin^3\beta + \tfrac{1}{2}(\cos(2\delta_S + 4\pi J)t_1 + \cos(2\delta_S - 4\pi J)t_1)(I_y(2 - 3S_z^2))\sin^3\beta. \quad (10)$$

Note the flip angle dependence of the various terms. This is to be compared with the flip angle dependence in the two-spin-1/2 system [27] given below:

$$I_x S_y + I_y S_x; \xrightarrow{(\delta_I I_z + \delta_S S_z + 2\pi J I_z S_z)t_1, \beta_x, \text{obs}} \rightarrow$$
$$(\cos(\delta_I + \delta_S)t_1)\sin\beta(I_x S_z + I_z S_x) + (\sin(\delta_I + \delta_S)t_1)\cos\beta\sin\beta(I_y S_z + I_z S_y). \quad (11)$$

Note also, incidentally, that the 'central' component of one-spin DQC, even if it could be prepared, is unobservable regardless of the reconversion pulse flip angle:

$$(S_y^2 - S_x^2) \xrightarrow{\beta_x} (\cos^2\beta)S_y^2 + (\sin^2\beta)S_z^2 - S_x^2 + (\sin\beta\cos\beta)[S_y, S_z]_+$$
$$\equiv (\sin^2\beta)(S_z^2 - S_y^2) + (S_y^2 - S_x^2) + (\sin\beta\cos\beta)[S_y, S_z]_+. \quad (12)$$

The coherence transfer process itself can be understood better by looking at the individual coherences rather than the whole density matrix. We make a detailed analysis of this coherence transfer process from the viewpoint of the energy level diagram shown in figure 2. In a two-spin-1 system there are 10 DQCs, which are listed in table 1, along with their frequencies.

From table 1 it may be noted that DQCs 1 and 4 correspond to 'outer' components of two-spin DQC, while 2 and 3 correspond to the doubly degenerate 'central' component of two-spin DQC. DQCs 5, 7, 8 and 10 correspond to the 'outer' components of one-spin DQC, while DQCs 6 and 9 are the 'central' component of the one-spin DQC, which is not created by the preparation sequence as seen from equation (6).

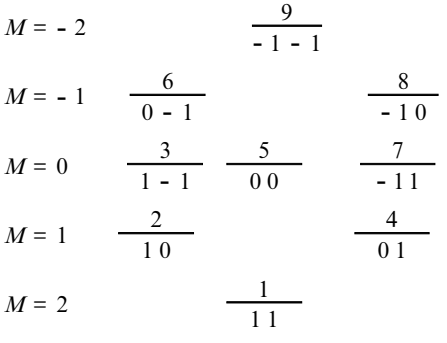

Figure 2. Energy level diagram of a two-spin-1 system.

Table 1. Double quantum coherences in the two-spin-1 AX system.

S. No.	DQC	Frequency
1	5×1	$\delta_I + \delta_S + 2\pi J$
2	8×4	$\delta_I + \delta_S$
3	6×2	$\delta_I + \delta_S$
4	9×5	$\delta_I + \delta_S - 2\pi J$
5	7×1	$2\delta_I + 4\pi J$
6	8×2	$2\delta_I$
7	9×3	$2\delta_I - 4\pi J$
8	3×1	$2\delta_S + 4\pi J$
9	6×4	$2\delta_S$
10	9×7	$2\delta_S - 4\pi J$

Table 2. Single quantum coherences in the two-spin-1 AX system.

S. No.	DQC	Frequency
1	7×4	$\delta_I + 2\pi J$
2	4×1	$\delta_I + 2\pi J$
3	8×5	δ_I
4	5×2	δ_I
5	9×6	$\delta_I - 2\pi J$
6	6×3	$\delta_I - 2\pi J$
7	3×2	$\delta_S + 2\pi J$
8	2×1	$\delta_S + 2\pi J$
9	6×5	δ_S
10	5×4	δ_S
11	9×8	$\delta_S - 2\pi J$
12	8×7	$\delta_S - 2\pi J$
13	7×2	$2\delta_I - \delta_S + 2\pi J$
14	6×7	$2\delta_I - \delta_S - 2\pi J$
15	3×4	$-\delta_I + 2\delta_S + 2\pi J$
16	8×3	$-\delta_I + 2\delta_S - 2\pi J$

There are 16 SQCs in this system. The SQCs along with their frequencies are listed in table 2.

The observable SQCs in a weakly coupled system are the first 12 SQCs of table 2. Note that this corresponds to the two multiplets of three components each centred at δ_I and δ_S, respectively, each component being doubly degenerate. SQCs 13–16, being combination coherences, are not observable in weakly coupled systems.

3. Simulation of the coherence transfer function

The coherence transfer function [24–26] quantifies the amplitude and phase of the transfer between any two coherences under the action of a mixing pulse. The coherence transfer function Z_{qrtu} for CT from a double quantum coherence tu to a single quantum coherence qr is given by

$$Z_{qrtu} = (R(\beta))_{qt} \times (R(\beta))^*_{ur}, \qquad (13)$$

where $R(\beta)$ is the rotation matrix for a mixing pulse of flip angle β. The rotation operator that corresponds to a resonant RF pulse along the interaction frame j axis with flip angle β for a spin-1 system is given by

$$(R_j(\beta)) = \exp(-i\beta I_j) = \cos(\beta I_j) - i\sin(\beta \mathbf{I}_j)$$
$$\equiv \mathbf{1} + (\cos\beta - 1)I_j^2 - i(\sin\beta)I_j. \qquad (14)$$

The corresponding matrix representation of $R_x(\beta)$ in the Zeeman basis is

R	$\lvert +\mathbf{1}\rangle$	$\lvert \mathbf{0}\rangle$	$\lvert -\mathbf{1}\rangle$
$\langle +\mathbf{1}\rvert$	$\frac{1}{2}(\cos\beta + 1)$	$\frac{-i}{\sqrt{2}}\sin\beta$	$\frac{1}{2}(\cos\beta - 1)$
$\langle \mathbf{0}\rvert$	$\frac{-i}{\sqrt{2}}\sin\beta$	$\cos\beta$	$\frac{-i}{\sqrt{2}}\sin\beta$
$\langle -\mathbf{1}\rvert$	$\frac{1}{2}(\cos\beta - 1)$	$\frac{-i}{\sqrt{2}}\sin\beta$	$\frac{1}{2}(\cos\beta + 1)$

The coherence transfer function in the general case of N weakly coupled, inequivalent spin-1 nuclei is therefore given by [17]:

$$Z_{qrtu} = i^{(N_s^{ru} - N_s^{qt})}(\cos\beta)^{(N_0^{qt} + N_0^{ru})}\left[\frac{(\cos\beta + 1)}{2}\right]^{(N_1^{qt} + N_1^{ru})}$$
$$\times \left[\frac{(\cos\beta - 1)}{2}\right]^{(N_d^{qt} + N_d^{ru})}\left(\frac{\sin\beta}{\sqrt{2}}\right)^{(N_s^{qt} + N_s^{ru})}, \qquad (15)$$

where N_s^{qt} indicates the number of spins which require a single quantum flip to convert state q to t, N_d^{qt} indicates the number of spins which require a double quantum flip to convert state q to t, N_0^{qt} indicates the number of spins having the same quantum number $m = 0$ in both the states q and t, and N_1^{qt} indicates the number of spins having the same quantum number $m \neq 0$ in both the states. Note that the spin state of each nucleus must belong to one of these four categories in the two states considered. For an N spin system this leads to the condition $N_s^{qt} + N_d^{qt} + N_0^{qt} + N_1^{qt} = N$. The form of the Z coefficients clearly follows from the matrix representation of **R**.

3.1. *Coherence transfer amplitude*

We have studied the coherence transfer function numerically. To this end, we have developed a 'Matlab' program (a listing may be obtained from the authors). In figures 3–5, we plot coherence transfer amplitude as a function of reconversion pulse flip angle β for transfer from DQC to various SQCs, with P-type double quantum selection.

While numerically simulating the amplitude we have accounted for degeneracy in both the DQCs as well as SQCs by adding together *complex* CT amplitudes in such cases. For example, the CT amplitude for the 'central' component of the two-spin DQC (C2DQ) to the central component of the SQC (CSQ_I), precessing with frequency δ_I is given by

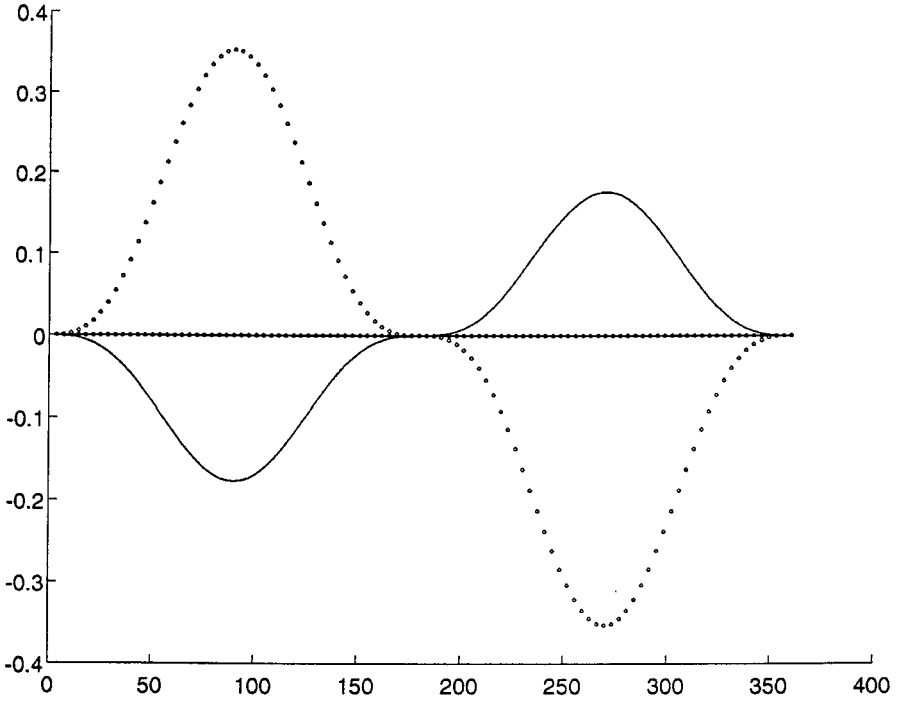

Figure 3. Simulation of the coherence transfer amplitude as a function of the reconversion pulse flip angle β, from one-spin DQC to various SQCs: dotted curve, CT amplitude for transfer to the central SQC component of the coupled spin; solid curve, CT amplitude for transfer to the outer SQC component of coupled spin; solid line with amplitude of zero gives the CT amplitude for transfer to the parent spin.

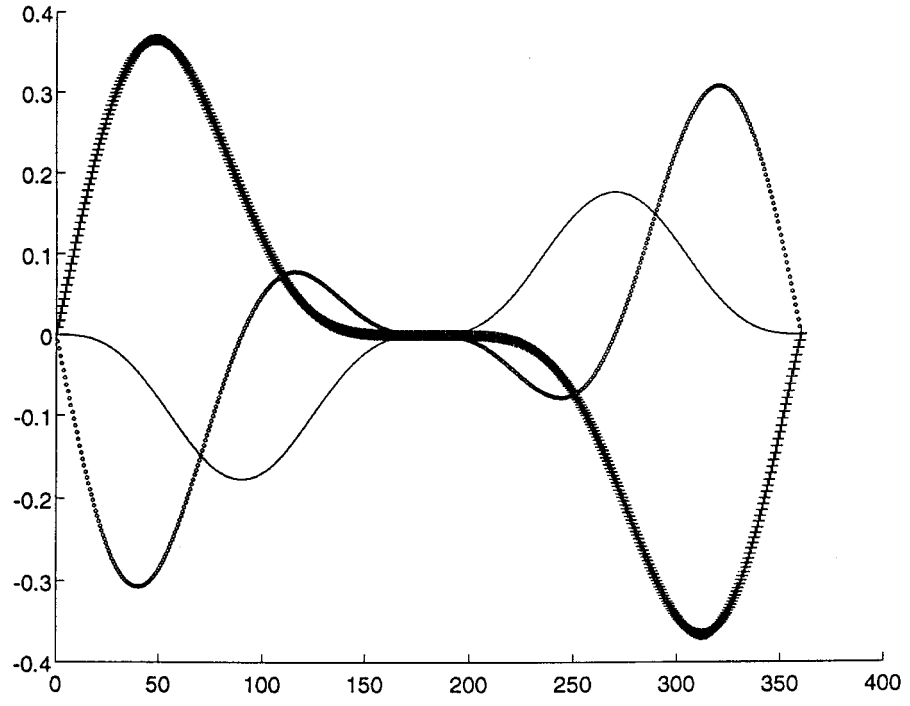

Figure 4. Simulation of the coherence transfer amplitude as a function of the reconversion pulse flip angle β, from 'outer' component of two-spin DQC (precessing with frequency $\delta_I + \delta_S + J$), to various SQCs: ·····, CT amplitude for transfer to the central SQC component (precessing with frequency δ_I or δ_S); +, CT amplitude for transfer to the connected outer SQC component with precession frequency $\delta_I + J$ or $\delta_S + J$; and solid line, CT amplitude for transfer to the remote outer SQC component with precession frequency $\delta_I - J$ or $\delta_S - J$.

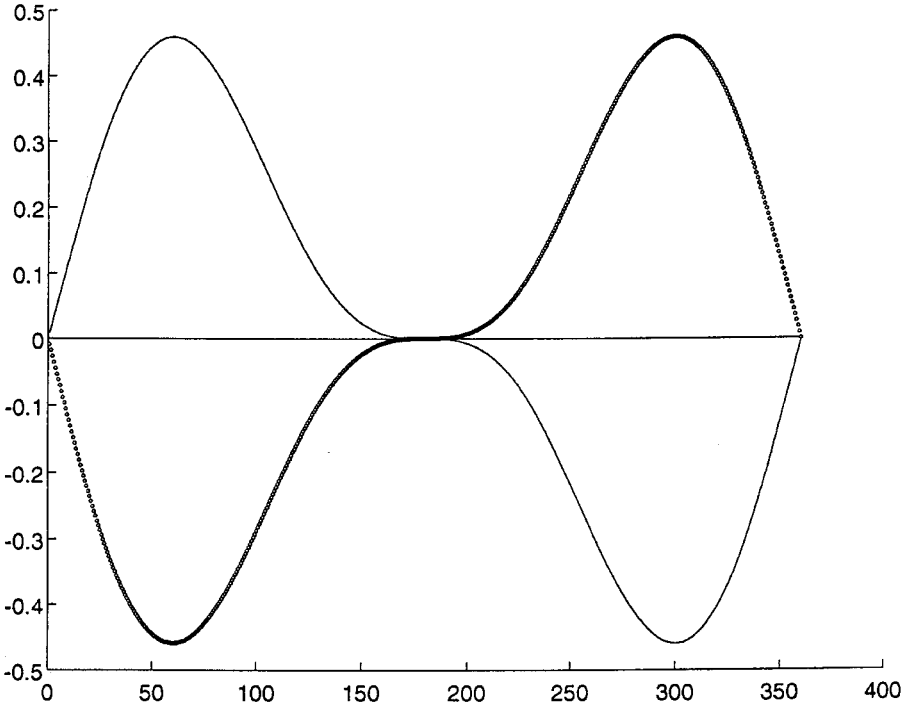

Figure 5. Simulation of the coherence transfer amplitude as a function of the reconversion pulse flip angle β, from 'central' component of two-spin DQC precessing with frequency $\delta_I + \delta_S$, to various SQCs: ·····, CT amplitude for transfer to one of the outer components of the SQC; and solid curve, CT amplitude for transfer to the other outer component of the SQC. Note that the amplitudes are equal and opposite. The solid line with an amplitude of zero gives the CT amplitude for transfer to the central component of the SQC.

$$Z_{\mathrm{CSQ}_I;\,\mathrm{C2DQ}} = Z_{8562} + Z_{5262} + Z_{8584} + Z_{5284}. \qquad (16)$$

From figures 3–5 we note that, unlike the situation with two-spins-1/2, here the coherence transfer amplitudes from DQCs to various SQCs are not equal.

3.1.1. *One-spin DQC*

From figure 3 we note that for one-spin DQC the coherence transfer amplitudes to outer components of single quantum multiplets are symmetric, but different

from the coherence transfer amplitude to the central component of the SQC. The maximum transfer occurs in both the cases for $\beta = 90^\circ$. Also note that the single quantum multiplet pattern that results on reconversion is a $(-1, 2, -1)$ triplet for any value of β.

3.1.2. *Two-spin DQC*

The response of two-spin DQC to mixing pulse flip angle is more complex.

(i) It can be seen from figure 4 that the 'outer' components of the two-spin DQC, with precession frequency $\delta_I + \delta_S \pm J$ are mixed asymmetrically to the multiplet components of the single quantum coherence. Clearly this relates to the fact that for two-spin DQC with precession frequency $\delta_I + \delta_S + J$, the directly connected transitions are δ_I, δ_S, $\delta_S + J$ and $\delta_I + J$ and, hence, for small values of β, the transfer of coherence is only to one of the outer components of the SQC, as seen from figure 4. Similar comments apply to the other component of the two-spin DQC with precession frequency $\delta_I + \delta_S - J$. These features may be understood from the series expansion of the coherence transfer amplitude as a function of β:

$$
\begin{aligned}
Z_{qrtu} &= (\exp(-\mathrm{i}\beta F_x))_{qt}(\exp(\mathrm{i}\beta F_x))_{ur} \\
&= \left(1 - \mathrm{i}\beta F_x + \frac{(\mathrm{i}\beta)^2}{2!}F_x^2 - \frac{(\mathrm{i}\beta)^3}{3!}F_x^3 \cdots\right)_{qt} \\
&\quad \times \left(1 + \mathrm{i}\beta F_x + \frac{(\mathrm{i}\beta)^2}{2!}F_x^2 - \frac{(\mathrm{i}\beta)^3}{3!}F_x^3 \cdots\right)_{ur} \\
&= \delta_{qt}\delta_{ur} + \mathrm{i}\beta(\delta_{qt}(F_x)_{ur} - \delta_{ur}(F_x)_{qt}) \\
&\quad + \frac{(\mathrm{i}\beta)^2}{2!}(\delta_{qt}(F_x)_{ur}^2 + \delta_{ur}(F_x)_{qt}^2 - 2(F_x)_{qt}(F_x)_{ur}) + \cdots \\
&= \delta_{qt}\delta_{ur} + \frac{\mathrm{i}\beta}{\sqrt{2}}(\delta_{qt}(\delta_{ur+1} + \delta_{ur-1}) - \delta_{ur}(\delta_{qt+1} + \delta_{qt-1})) \\
&\quad + \frac{1}{2!}\left(\frac{\mathrm{i}\beta}{\sqrt{2}}\right)^2(\delta_{qt}(\delta_{ur+2} + \delta_{ur-2} - 2\delta_{ur}) \\
&\quad + \delta_{ur}(\delta_{qt+2} + \delta_{qt-2} - 2\delta_{qt}) \\
&\quad - 2(\delta_{qt+1}(\delta_{ur+1} + \delta_{ur-1}) + \delta_{qt-1}(\delta_{ur+1} + \delta_{ur-1}))) + \cdots .
\end{aligned}
\tag{17}
$$

Using the constraints that tu is a double quantum coherence, i.e., $t - u = 2$ and qr is a single quantum coherence, i.e., $q - r = 1$, we observe the following. (1) The first term is a product of two delta functions and exists only when $q = t$ *and* $r = u$; hence it vanishes in this case. (2) The second term which is linear in β exists when one of the delta functions exists, i.e., when $q = t$ *and* $u = r \pm 1$; *or* $u = r$ *and* $q = t \pm 1$; when $q = t$ we have $u = r - 1$ and the value of this term is $k = \mathrm{i}\beta/\sqrt{2}$; when $u = r$ we have $q = t - 1$ and the value of this term is $-k$. (3) The third term also vanishes when $q = t + 1$, $u = r$; *and* when $q = t - 1$, $u = r - 2$. Therefore for values of mixing pulse flip angle β selected such that terms in β^3 may be neglected, coherence is transferred only when there is a common level between qr and tu. We may employ

$$
\frac{(3!)(\beta/\sqrt{2})}{3(\beta/\sqrt{2})^3} > 6, \quad \text{i.e., } \beta^2 < \tfrac{2}{3}
$$

as the cut-off condition for cubic and higher order terms in β.

(ii) The coherence transfer amplitude for transfer from 'outer' components of two-spin DQC to the remote and connected outer SQ components are maximized, respectively, for $\beta = 270^\circ$ and $\beta = 48{\cdot}6^\circ$. Further, these maximum amplitudes are unequal. The coherence transfer amplitude for transfer to the central SQC component is maximized for $\beta = 40^\circ$; also note in this case that the coherence transfer amplitude crosses zero for $\beta = 90^\circ$; at this flip angle the amplitudes of transfer to the two outer components of an SQ multiplet become equal and opposite.

(iii) In the case of the 'central' component of the two-spin DQC precessing with frequency $\delta_I + \delta_S$ during the evolution period, coherence is not transferred to the central SQC component. It may be noted from figure 5 that transfer amplitudes to the outer SQ components are equal and opposite for all values of β. This behaviour of the CT amplitude is similar to that in the case of the two-spin-1/2 system [27]. This is due to the fact that this is the sole DQC component in the two-spin-1 system which is independent of J, as is the case in the two-spin-1/2 system. Predictably in this sense, the coherence transfer amplitude is maximized for $\beta = 60^\circ$.

'SMART' [28] simulations of 2D-DQS were performed for $\beta = 40^\circ$ and $\beta = 48{\cdot}6^\circ$. It can be seen from the row spectrum in figure 6, corresponding to the 'outer' component of two-spin DQC, that the amplitudes of the outer SQC components are indeed unequal.

3.2. *Coherence transfer echoes and anti-echoes*

We next inquire into the behaviour of CT echo and anti-echo amplitudes.

We plot the DQ coherence transfer echoes in figures 7–9. The echo plot is generated by summing the *absolute magnitude* of the CT amplitude from a DQC to various SQCs. For example, the CT echo plot for 'central' component of two-spin DQC is generated as follows:

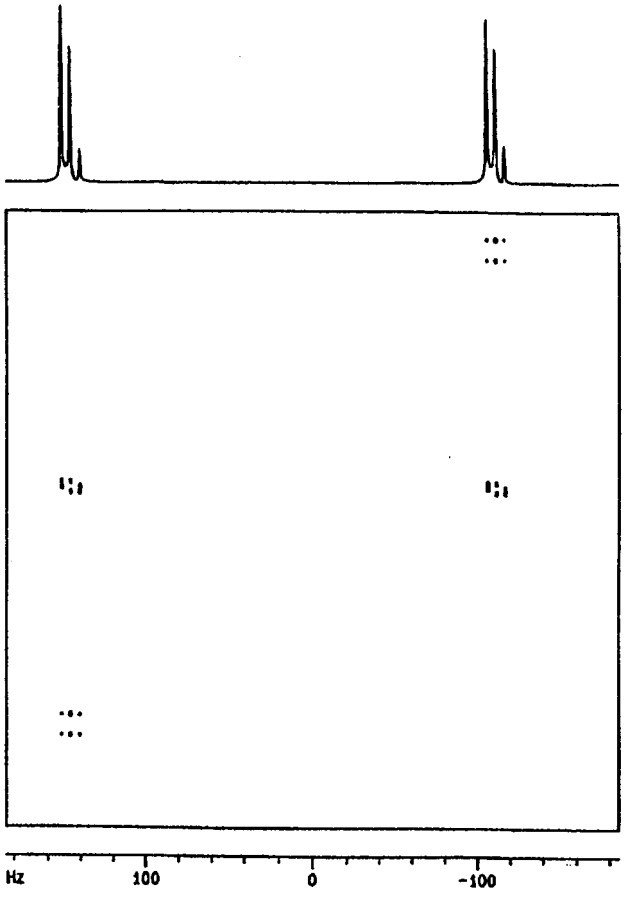

Figure 6. 'SMART' simulation of the double quantum spectrum for a reconversion pulse flip angle of 40° with P-type double quantum pathway selection. The 1D spectrum corresponds to the row spectrum of the two-spin DQC with precession frequency $\delta_I + \delta_S + J$.

$$Z = |Z_{\mathrm{CSQ}_I;\,\mathrm{C2DQ}}| + |Z_{\mathrm{O1SQ}_I;\,\mathrm{C2DQ}}| + |Z_{\mathrm{O2SQ}_I;\,\mathrm{C2DQ}}| + |Z_{\mathrm{CSQ}_S;\,\mathrm{C2DQ}}| + |Z_{\mathrm{O1SQ}_S;\,\mathrm{C2DQ}}| + |Z_{\mathrm{O2SQ}_S;\,\mathrm{C2DQ}}|. \quad (18)$$

CSQ_I refers to central SQC component with precession frequency δ_I, $\mathrm{O1SQ}_I$ refers to the outer SQC component with precession frequency $\delta_I + J$, $\mathrm{O2SQ}_I$ refers to the outer SQC component with precession frequency $\delta_I - J$, and C2DQ refers to the 'central' component component of two-spin DQC.

Unlike the situation in the case of the two-spin-1/2 system [27], there are three different coherence transfer echoes: one corresponding to the 'outer' component and a second to the 'central' component of the two-spin DQC, and a third corresponding to one-spin DQC.

It can be noted from figure 7 that for one-spin DQC the maxima of the echo amplitude and the anti-echo amplitude are achieved with a reconversion pulse flip angle of 90°. This results in maximizing the sensitivity

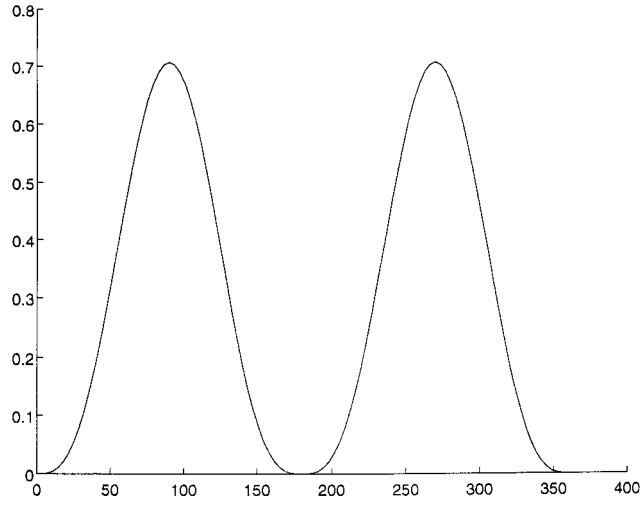

Figure 7. Simulation of the CT amplitude of one-spin DQC echo/anti-echo as a function of reconversion pulse flip angle β.

for both the pathways at the same value of $\beta = 90°$. Hence the pure phase TPPI spectrum of one-spin DQC also results in optimum sensitivity (unlike the two-spin-1/2 situation, where there is a trade-off of sensitivity under TPPI [27]).

In the case of two-spin DQC we have two different optimum reconversion pulse flip angles, one for maximizing the CT echo magnitude for transfer from 'outer' components of DQC and another for transfer from the 'central' component of DQC. It can be seen from figures 8 and 9 that the echoes and the anti-echoes have the maximum sensitivity for $\beta = 40°$ and $\beta = 140°$, respectively, for transfer from 'outer' components of DQC, while maximum sensitivity is achieved at $\beta = 60°$ and $\beta = 120°$ for transfer from the 'central' component of DQC.

The reconversion pulse flip angle for optimal N/P suppression ratio for all the two-spin DQC components is found to be $\beta = 135°$, which is the same for a two-spin-1/2 system [27].

4. Experiment and discussion

A system of two equivalent spin-1/2 nuclei has composite angular momentum states with $I = 0$ and $I = 1$. Since $I = 0$ is a non-magnetic state, such a two-spin-1/2 system is homomorphic with a spin-1 system. One may thus apply the results we have for the two-spin-1 system, *mutatis mutandis*, to a spin-1/2 A_2X_2 system. Indeed, all our 'Matlab' simulations of CT involving DQCs are exactly similar for both the nine-level two-spin-1 system and the 16-level spin-1/2 A_2X_2 system. This may be understood readily on the basis that: (i) the $I = 0$ composite angular momentum state cannot by

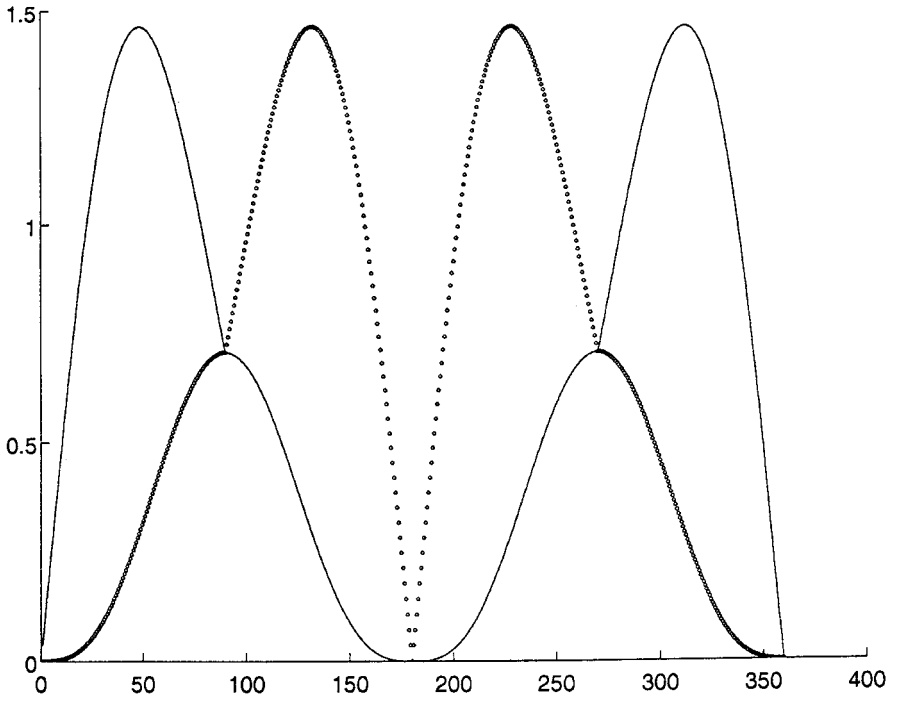

Figure 8. Simulation of the CT amplitude of two-spin DQC with precession frequencies $\pm(\delta_I + \delta_S)$, as a function of reconversion pulse flip angle β: solid line, CT amplitude for echo; and dotted curve/thick line, CT amplitude for anti-echo.

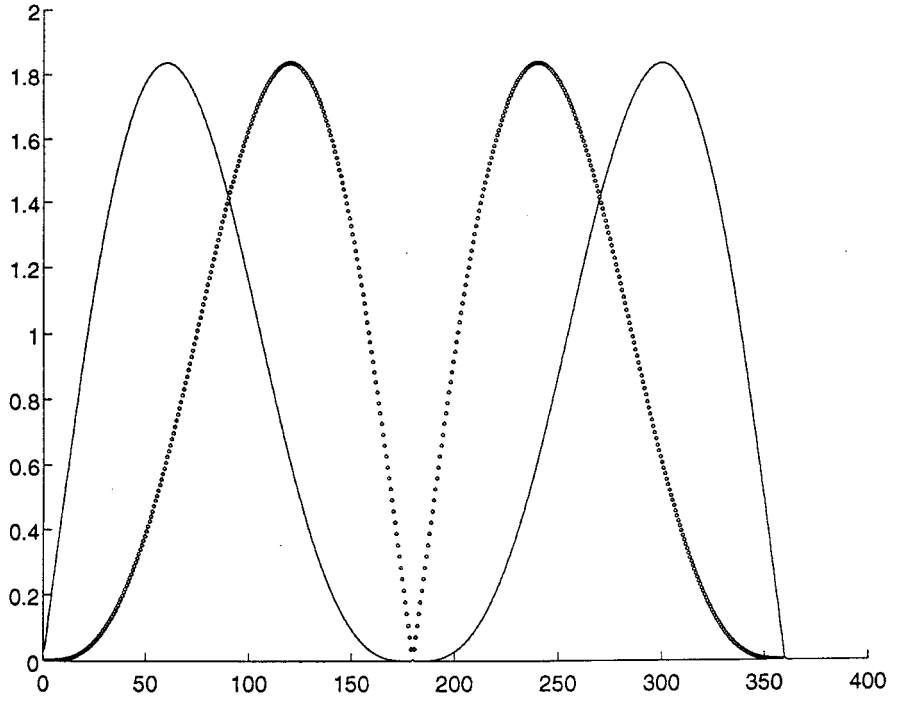

Figure 9. Simulation of the CT amplitude of two-spin DQC with precession frequencies $\pm(\delta_I + \delta_S \pm J)$, as a function of reconversion pulse flip angle β: solid line, CT amplitude for echo; and ·····, CT amplitude for anti-echo.

definition participate in two-spin DQC: and (ii) one-spin DQC may be prepared in solution state only by virtue of non-zero coupling to a second spin, which again requires $I \neq 0$. Barring relaxation effects, therefore, and focusing on the DQ-CT behaviour, we may exploit this equivalence. We experimentally demonstrate the results on 2-aminoethanol in D_2O, this system being a good approximation to an A_2X_2 spin system at 300 MHz. (We have ascertained this by the fact that there is little observable transfer to the parent group from the A_2 or X_2 one-group double quantum coherence: significant transfer to the parent group is characteristic of an AA′XX′

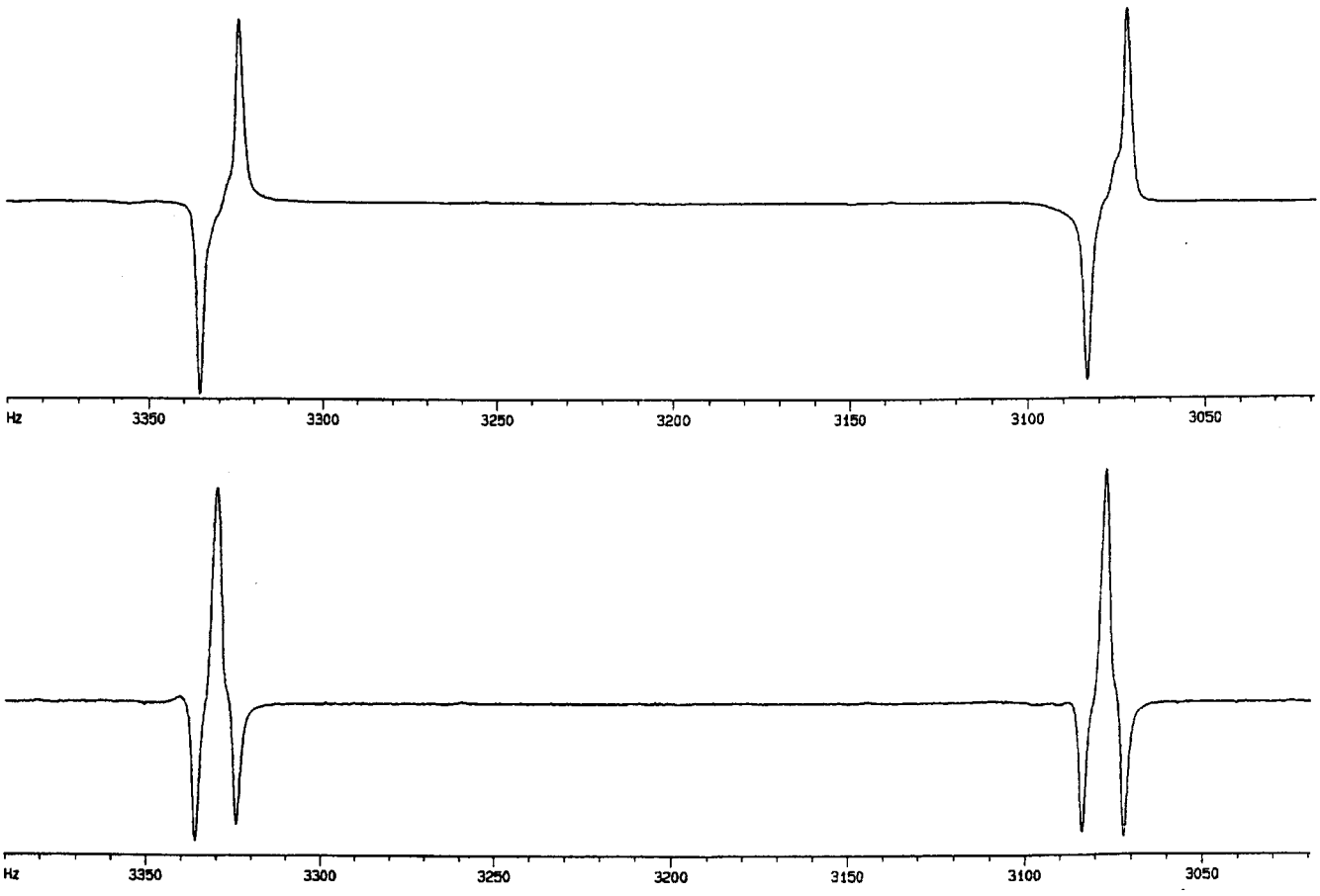

Figure 10. Experimental proton spectra of the DQ*J* filter experiment on 2-aminoethanol. The top trace corresponds to two-spin DQC selection, obtained for $t_1 = 21{\cdot}78$ ms $(1/8J)$, and the bottom trace corresponds to one-spin DQC selection, resulting from the choice of $t_1 = 87$ ms $(1/2J)$.

system. Work on the theoretical and experimental implications of magnetic inequivalence on multiple quantum spectroscopy is in progress and includes consideration of these aspects, which have been observed earlier in deuterium DQS [17]. We may further note the analogy with 3-aminopropanol, which has been treated as an $A_2M_2X_2$ system by Ernst *et al.* [26] in the context of multiple quantum spectroscopy.) The spectra were obtained on a Bruker MSL300P NMR spectrometer. The DQ*J* filter experiment with preparation resulting in both kinds of DQCs was performed with the DQ*J* filter pulse sequence of figure 1. It can be seen from figure 10 that for $t_1 = 1/(8J)$, $(J = 5{\cdot}42$ Hz), two-spin DQC gets separated, resulting in a neat anti-phase $(-1, 0, 1)$ doublet as predicted by equation (4). On the other hand, one-spin DQC gets separated at $t_1 = 1/(2J)$, resulting in an anti-phase $(-1, 2, -1)$ triplet as predicted by equation (4). Figure 11 shows the pure phase 2D double quantum spectrum of 2-aminoethanol. The spectrum was run with a mixing pulse of 90°, in TPPI mode. It is to be emphasized that this spectrum has exactly the same appearance and multiplet patterns as predicted and observed for the double quantum spectrum of two-spin-1 systems [13, 19], including [3,3′-D_2]-norcamphor, and [3,3′-D_2]-camphor, where the homonuclear ^2H–^2H couplings involved are well below 0·4 Hz; further, clusters of organolithium species with homonuclear ^6Li–^6Li couplings below 0·25 Hz [19] behave as predicted.

For reconversion pulse flip angle ≠ 90° the 2D double quantum spectra were run with gradient controlled pathway selection using a 5 mm RF insert in an actively shielded micro-imaging probe head. The double quantum pathway selection was effected by applying *z* gradient pulses immediately before and after the reconversion pulse, the amplitudes being in the ratio $1 : -2$ (P-type selection). Gradient amplitudes are $2{\cdot}33$ G cm^{-1} and $-4{\cdot}66$ G cm^{-1}. The experimental plots shown in figures 12–14 confirm all the detailed predictions of the theory and simulations of CT amplitudes in figures 3–5 and echo plots of figures 7–9.

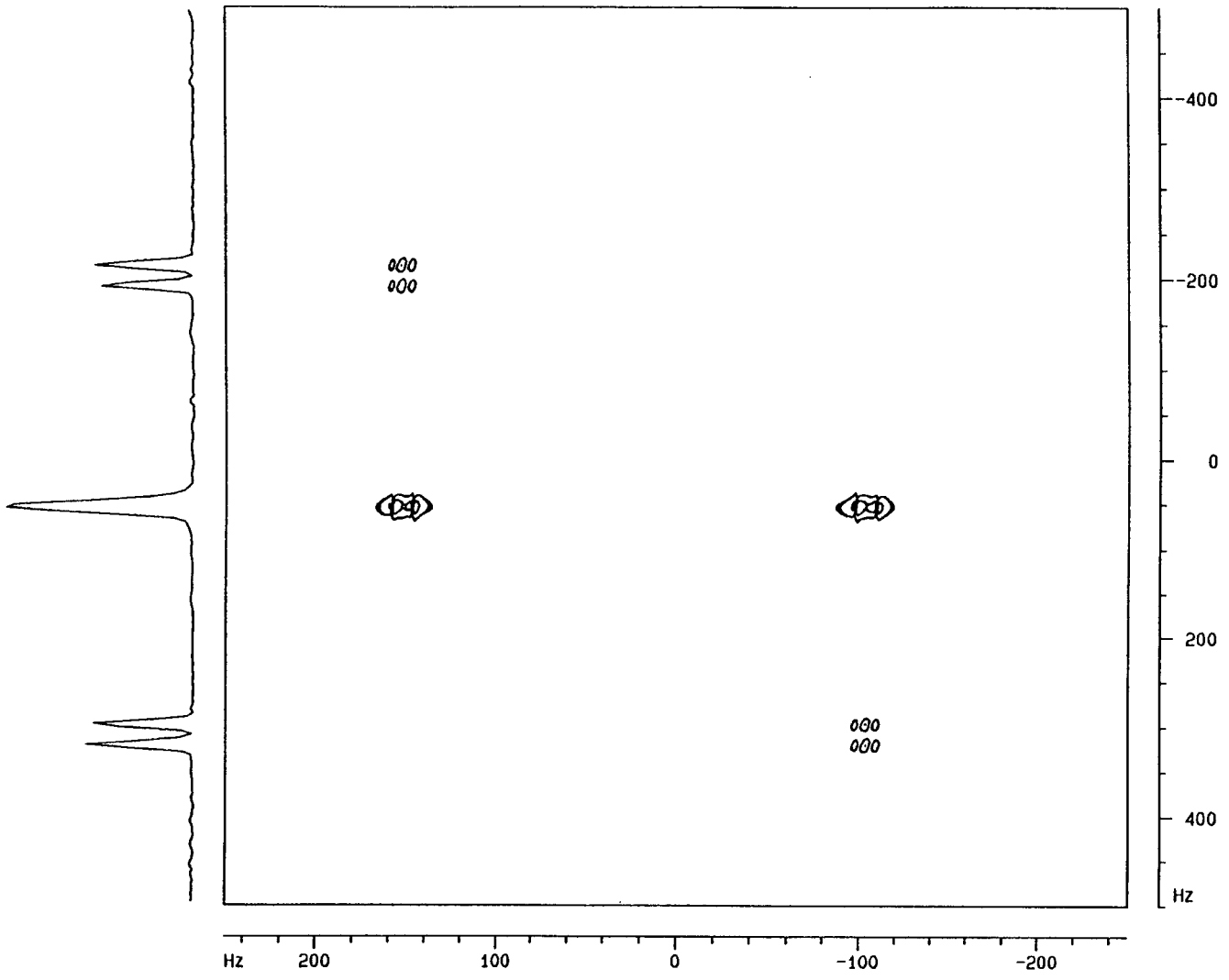

Figure 11. Experimental 2D pure phase double quantum spectrum of 2-aminoethanol. The amplification of coupling in the case of one-spin DQC can be seen clearly from the F_1 projection shown. Though the triplet of the two-spin DQC is unresolved the doublet of the one-spin DQC is resolved neatly down to the baseline.

5. Conclusion

We have investigated in detail coherence transfer involving DQCs in a two-spin-1 system. We have shown that the evolution of the two kinds of DQCs under homonuclear coupling provides a recipe for their separation. We have introduced a double quantum J filter sequence for the separation of the two kinds of DQCs and have verified the results experimentally on a spin-1/2 system that mimics the two-spin-1 AX system.

We have presented in detail the coherence transfer process for an arbitrary reconversion pulse flip angle β. Based on simulations and experimental verification of CT amplitudes, we note the following.

(1) The behaviour of the coherence transfer amplitude as a function of β is different for one-spin DQC, the 'outer' components of two-spin DQC, and the 'central' component of two-spin DQC. The CT amplitude from each DQC to various SQC components is also different. (a) CT amplitudes from the 'outer' components of one-spin DQC to the outer SQC components are equal, being the negative one half of that to the central component of SQC. In all these cases the CT amplitude is maximized for $\beta = 90^\circ$. The CT amplitude for transfer from the 'central' component of one-spin DQC to any SQC component vanishes identically. (b) CT amplitudes from 'outer' two-spin DQC components to the connected and the remote outer components of SQC are asymmetric and are maximized for $\beta = 48{\cdot}6^\circ$ and $\beta = 90^\circ$, respectively. The CT amplitude for transfer to the central SQC component is maximized for $\beta = 40^\circ$. The CT amplitude for transfer from the 'central' component of two-spin DQC to outer SQC components are

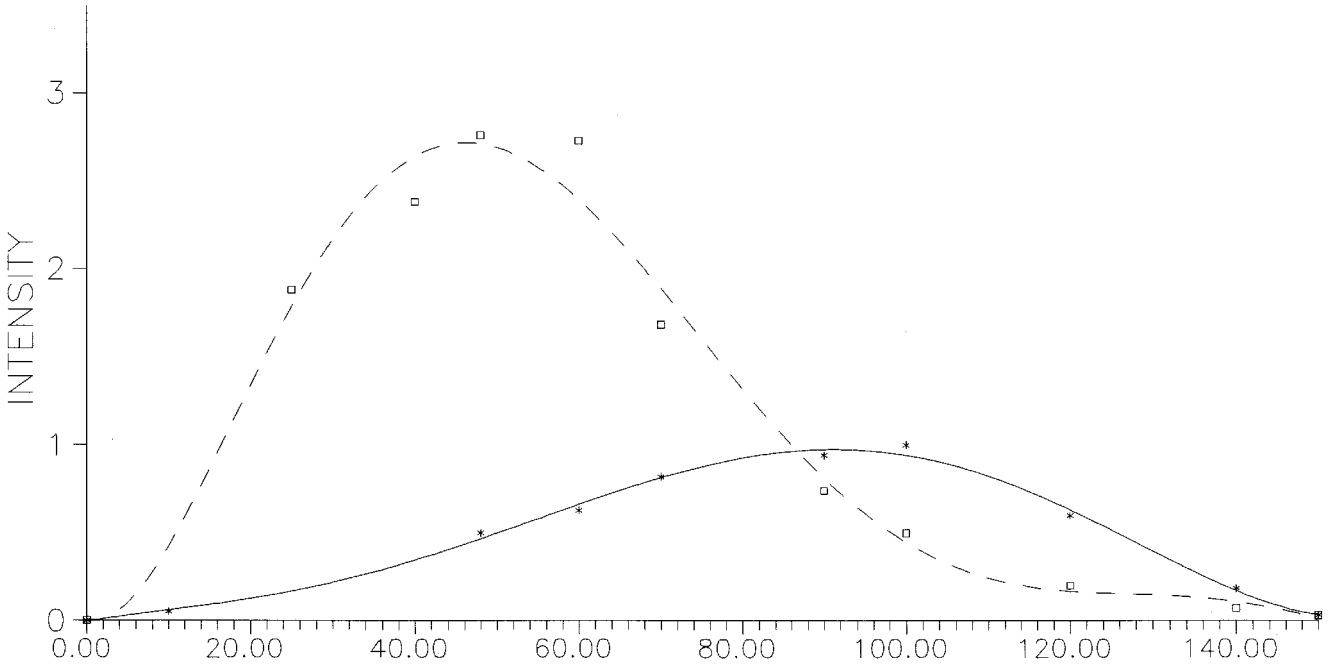

Figure 12. Experimental coherence transfer intensity as a function of the reconversion pulse flip angle β, from 'outer' component of two-spin DQC (precessing with frequency $\delta_I + \delta_S + J$), to various SQCs: □, data points of CT intensity for transfer to the connected outer SQC component with precession frequency $\delta_I + J$ or $\delta_S + J$; and *, data points of CT intensity for transfer to the remote outer SQC component with precession frequency $\delta_I - J$ or $\delta_S - J$. The broken and continuous curves connecting the experimental data points are polynomial fits of the data points and do not have any theoretical significance.

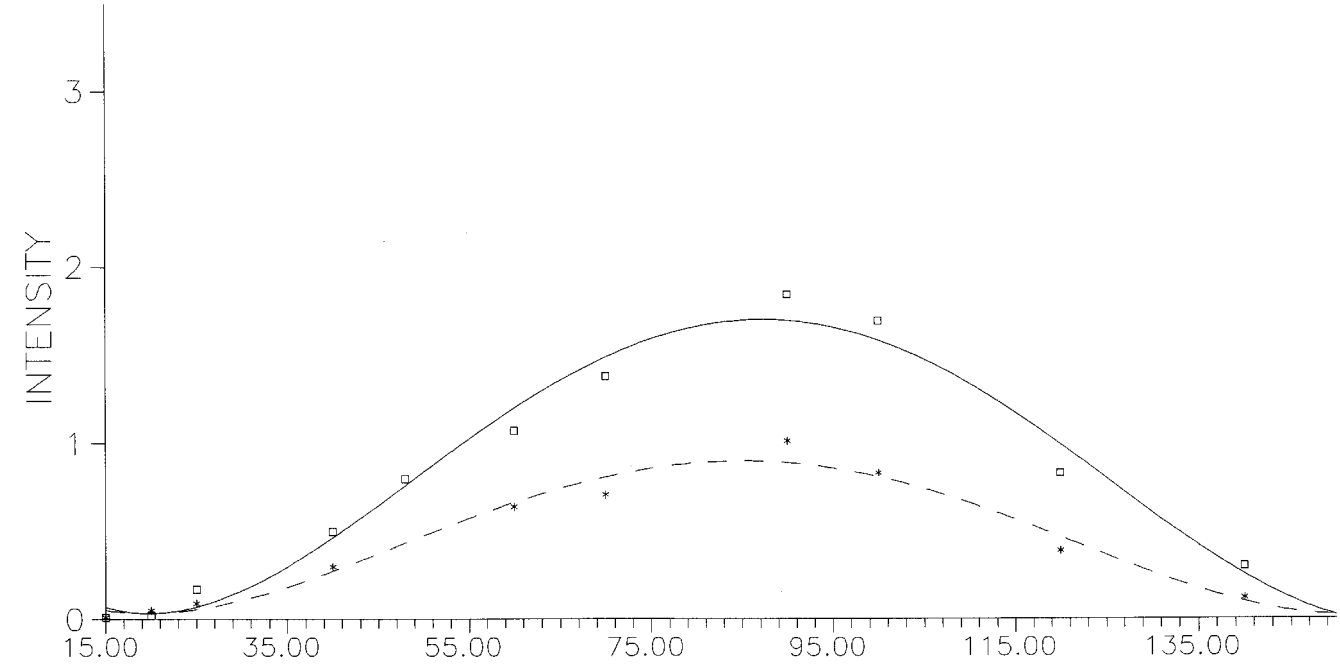

Figure 13. Experimental coherence transfer intensity as a function of the reconversion pulse flip angle β, from the 'outer' component of one-spin DQC to various SQCs: □, data points of CT intensity for transfer to the central SQC component of the coupled spin; and *, data points of CT intensity for transfer to the outer SQC components of the coupled spin. The solid and broken curves are polynomial fits of the experimental data points, and do not have any theoretical significance.

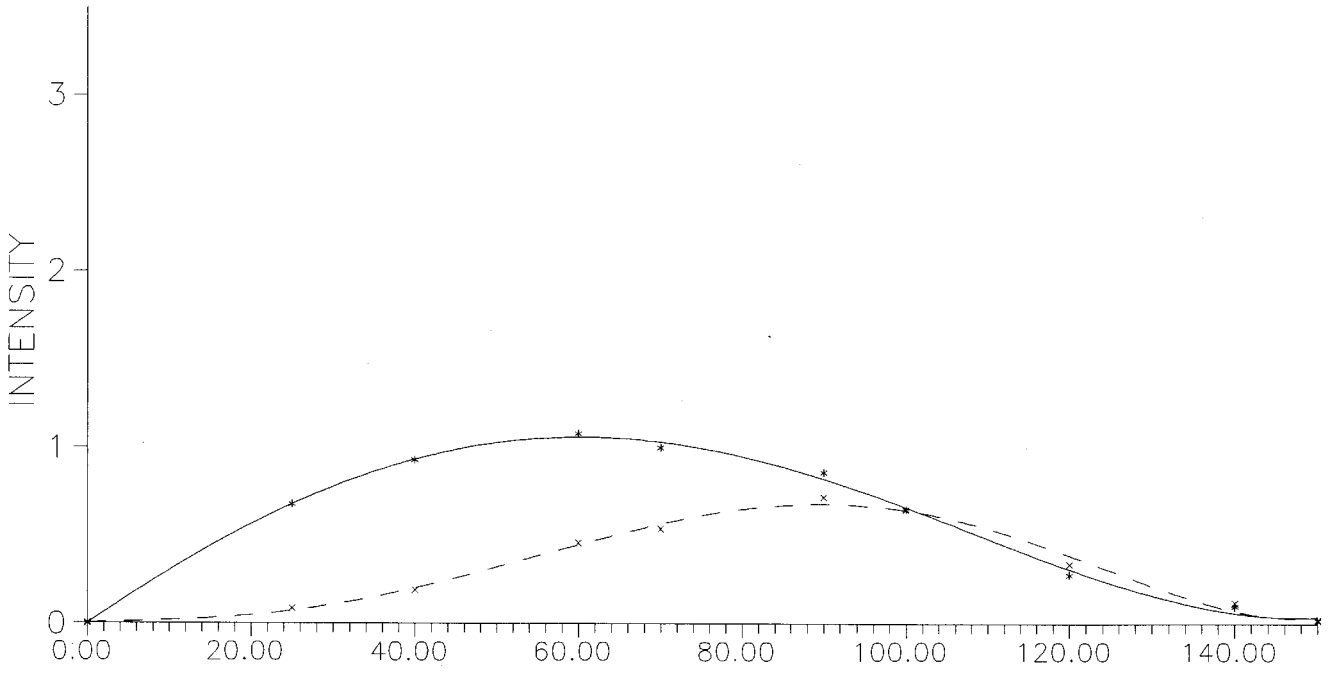

Figure 14. Experimental CT echo intensity as a function of reconversion pulse flip angle β: *, data points of CT intensity for 'central' component of two-spin DQC echo; and ×, data points of CT intensity for 'outer' component of one-spin DQC echo. The solid and broken lines are polynomial fits of the data points and have no theoretical significance.

equal and opposite for all values of β, with a maximum at $\beta = 60^\circ$, while that to the central component of the SQC is zero.

(2) There are three different coherence transfer echoes: two for two-spin DQC and one for one-spin DQC. (a) In the case of one-spin DQC, the echo and anti-echo extremum occurs at the same angle 90°; hence the pure phase spectrum of one-spin DQC does not compromise sensitivity, unlike the case of the two-spin-1/2 system. (b) In the case of 'outer' components of two-spin DQC, echo and anti-echo extremum occurs at reconversion pulse flip angles of 40° and 140°, respectively. On the other hand, the CT echo and anti-echo for 'central' component of two-spin DQC is maximized for $\beta = 60^\circ$ and 120°, respectively, which is identical to the situation with the two-spin-1/2 system. The close similarity between DQC in a two-spin-1/2 system and the 'central' component of two-spin DQC in a two-spin-1 system is noteworthy.

The present approach yields readily to a detailed examination of single, triple and four quantum spectroscopy of the two-spin-1 AX system as well. The same formalism can also be extended readily to N-spin-1 systems and can be modified easily to take into account magnetic inequivalence, as well as strong coupling effects.

S.V.R. thanks CSIR for a Senior Research Fellowship. N.C. acknowledges with pleasure the motivation for this work from a collaboration with Professor H. Günther, Universität Siegen, Germany.

References

[1] Schäublin, S., Höhener, A., and Ernst, R. R., 1974, *J. magn. Reson.*, **13** 196.
[2] Jacobsen, J. P., Bildsøe, H. K., and Schaumberg, K., 1976, *J. magn. Reson.*, **23,** 153.
[3] Stoll, M. E., Wolff, E. K., and Mehring, M., 1978, *Phys. Rev.* A, **17,** 1561.
[4] Pines, A., Ruben, D. J., Vega, S., and Mehring, M., 1976, *Phys. Rev. Lett.*, **36,** 110; Vega, S., Shattuck, T.W., and Pines, A., 1976, *Phys. Rev. Lett.*, **37,** 43.
[5] Vold, R. L., and Vold, R. R., 1977, *J. chem. Phys.*, **66,** 4018.
[6] Barbara, T. M., Vold, R. R., Vold, R. L., and Neubert, M. E., 1985, *J. chem. Phys.*, **82,** 1612.
[7] Spiess, H. W., 1978, *NMR Basic Principles and Progress*, Vol. 15, edited by P. Diehl, E. Fluck and R. Kosfeld (Berlin: Springer-Verlag), p. 55.
[8] Boden, N., Clark, L. D., Houlon, S. M., and Martimer, M., 1978, *Faraday Symp. chem. Soc.*, **109,** 1979.
[9] Spiess, H. W., 1985, *Adv. Polymer Sci.*, **66,** 24.
[10] Boeffel, C., Luz, Z., Poupko, R., and Zimmermann, H., 1989, *J. magn. Reson.*, **85,** 325.
[11] Tycko, R., Stewart, P. L., and Opella, S. J., 1986, *J. Amer. chem. Soc.*, **108,** 5419.

[12] Dong, R. Y., Friesen, L., and Richards, G. M., 1994, *Molec. Phys.*, **81,** 1017.
[13] Chandrakumar, N., 1996, *NMR Basic Principles and Progress*, Vol. 34, edited by P. Diehl, E. Fluck, R. Kosfeld, H. Günther and J. Seelig (Berlin: Springer-Verlag).
[14] Rinaldi, P. L., and Baldwin, N., 1982, *J. Amer. chem. Soc.*, **104,** 5791; 1983, *J. Amer. chem. Soc.*, **105,** 7523; Chandrakumar, N., 1984, *J. magn. Reson.*, **60,** 28; 1985, *J. magn. Reson.*, **63,** 174.
[15] Wesener, R., Schmitt, P., and Günther, H., 1982, *Org. magn. Reson.*, **22,** 468; Wesener, J. R., and Günther, H., 1985, *J. Amer. chem. Soc.*, **107,** 1537.
[16] Chandrakumar, N., and Ramamoorthy, A., 1992, *J. Amer. chem. Soc.*, **114,** 1123.
[17] Chandrakumar, N., 1993, *J. Amer. chem. Soc.*, **115,** 3780.
[18] Eppers, O., Fox, T., and Günther, H., 1992, *Helv. chim. Acta*, **75,** 883; Mons, H.-E., Bergander, K., and Günther, H., 1993, *Magn. Reson. Chem.*, **31,** 509.
[19] Chandrakumar, N., Mons, H-E., Hüls, D., and Günther, H., 1996, *Magn. Reson. Chem.*, **34,** 715.
[20] Hore, P. J., Zuiderweg, E. R. P., Nicolay, K., Dijkstra, K., and Kaptein, R., 1982, *J. Amer. chem. Soc.*, **104,** 4286; Bax, A., Freeman, R., and Kempsell, S. P., 1980, *J. Amer. chem. Soc.*, **102,** 4849; Nakai, T., and McDowell, C. A., 1993, *Molec. Phys.*, **79,** 965; 1994, *Molec. Phys.*, **81,** 337.
[21] Sørensen, O. W., Levitt, M. H., and Ernst, R. R., 1983, *J. magn. Reson.*, **55,** 104.
[22] Levitt, M. H., and Ernst, R. R., 1983, *Chem. Phys. Lett.*, **100,** 119; Levitt, M. H., and Ernst, R. R., 1985, *J. chem. Phys.*, **83,** 3297.
[23] Drobny, G., Pines, A., Sinton, S., Weitekamp, D. P., and Wemmer, D., 1979, *Symp. Faraday Soc.*, **13,** 49.
[24] Braunschweiler, L., Bodenhausen, G., and Ernst, R. R., 1983, *Molec. Phys.*, **48,** 535.
[25] Aue, W. P., Bartholdi, E., and Ernst, R. R, 1976, *J. chem. Phys.*, **64,** 2229.
[26] Ernst, R. R., Bodenhausen, G., and Wokaun, A., 1987, *Principles of Nuclear Magnetic Resonance in One and Two Dimensions* (Oxford: Clarendon Press).
[27] Mareci, T. H., and Freeman, R., 1982, *J. magn. Reson.*, **48,** 158.
[28] Studer, W., 1988, *J. magn. Reson.*, **77,** 424.